Domain-Boundary Structure of Styrene–Isoprene Block Copolymer Films Cast from Toluene Solutions[1a]

Takeji Hashimoto, Kikuo Nagatoshi,[1b] Akira Todo,[1c] Hirokazu Hasegawa,[1d] and Hiromichi Kawai*

Department of Polymer Chemistry, Faculty of Engineering, Kyoto University, Kyoto 606, Japan.
Received October 18, 1974

ABSTRACT: The domain structures of polystrene–polyisoprene A–B-type block copolymer films cast from toluene solutions were investigated by means of electron microscope and small-angle X-ray scattering (SAXS). The copolymers studied are those having fractions of A and B sequences which give rise to the domain structure of alternating lamellae of A and B components. The SAXS data which indicated that the lamellae are oriented almost parallel to the surfaces of the cast films were analyzed by using a current SAXS theory for a system having one-dimensional electron density variations. The analyses gave quantitative informations of the domain structure, (i) domain-boundary structure between A- and B-lamellae, *i.e.*, the electron density profile in the transition region from one lamella to another which is related to a degree of partial mixing of A and B block chains at the boundary and/or segment density distributions of the A and B block chains around their chemical junction points, (ii) uniformity of the domain size and regularity of mutual arrangement of the domains, and (iii) size of "grain" in which orientation of the domains are coherent. Effects of molecular weight of the block copolymers and annealing of the *as*-cast specimens at various temperatures were also studied. It was pointed out that total reflection of X-ray beams at sample–air interfaces affects, in some cases, the SAXS intensity distributions. A method to correct the total reflection was proposed.

Thermodynamic incompatibilities of A and B block chains of A–B- and A–B–A-type block copolymers have been shown to involve the microphase separation at the critical micelle concentration.[2a,b] The micelle structures formed are believed to be essentially maintained through the solvent evaporation process to result in the domain structures observed in solid films.[2b-4] The shape and size of the micelle or the domain have been analyzed thermodynamically, and have been shown to depend upon the incompatibility of molecules constituting the graft or the block copolymer, molecular weight, chemical composition, solvent used for casting, and temperature of casting.[3,5-10]

In this paper an attempt is made to analyze quantitatively the domain structure by means of the SAXS and electron microscopic observations with a hope of correlating the results with some thermodynamic properties of domain formation of A–B-type block copolymers.

Test Specimens

Two types of styrene–isoprene A–B-type block copolymers were synthesized according to the method described in the previous paper.[3] These are denoted as SI-H and SI-L specimens for convenience; the weight per cents of polystyrene are 43 and 59, and the total number-average molecular weights are 53.8×10^4 and 10.5×10^4 for the SI-H and SI-L specimens, respectively.

The copolymers were cast into films about 100 μ thick by pouring 5% toluene solution onto a glass plate floating on mercury, and by evaporating the solvent very gradually at 30° for a few days. The film specimens thus formed were further dried under a vacuum (10^{-6} mm) for several days until the samples were at constant weight. The *as*-cast films thus prepared were further annealed at temperatures below and above T_g (glass transition temperature) of polystyrene block under a vacuum of 10^{-6} mm for 25 hr. There was no detectable change in weight before and after annealing the samples. The T_g's measured with the torsion pendulum method are *ca.* 90° (for polystyrene block) and *ca.* 0° (for polyisoprene block) at *ca.* 0.1 Hz for the SI-H and -L specimens.

Experimental Results

Electron Micrographs. In Figure 1 are shown electron micrographs of ultra-thin sections of the specimens stained by osmium tetroxide. The dark phase corresponds to the stained polyisoprene phase, while the white phase corresponds to the polystyrene phase. The domain structures of the SI-L (left) and SI-H (right) specimens are shown to be alternating lamellae of polystyrene and polyisoprene phase as expected from the chemical compositions and the casting solvent.[3]

It is seen clearly that the domain structure of the copolymer having higher molecular weight (SI-H) is much more irregular than that having lower molecular weight (SI-L), and that the inter-lamellar spacing is greater for the SI-H specimens than for the SI-L specimens. Close observations of the micrographs indicate that thickness of each lamellar and thus the inter-lamellar spacing expand upon annealing the *as*-cast films at 108°, a temperature a little higher than the T_g of polystyrene. The degree of expansion of the lamellae is seen to be greater for the polyisoprene phase than for the polystyrene phase. The size of the grain in which the orientation of the domains is coherent is shown to be greater for the SI-L than for the SI-H.

Small-Angle X-Ray Scattering (SAXS). a. Collimating System. The SAXS photographs were taken with a Rigaku-Denki D-6C X-ray generator with a power of 40 kV, 20 mA. The patterns were taken by using point focusing and by using the collimating system; the second pinhole, specimen and camera were placed at 300, 320, and 620 mm from the first pinhole, respectively, and the diameters of the first and the second pinholes are 0.5 and 0.2 mm, respectively.

The SAXS intensity distributions were measured with a scintillation counter and a Rigaku-Denki Rotaflex RU-100PL with a power of 50 kV and 100 mA, and with line focusing under the following collimating system: the second slit, the third slit, the specimen and the receiving slit were placed at 249, 290, 310, and 610 mm from the first slit, respectively, and the sizes of the first, second, solar, and receiving slits are 0.1×10, 0.05×10, 0.1×15, and 0.05×15 mm^2, respectively. The intensity of scattered X-rays was high enough to be measured by using a counting-rate meter. The intensity was measured with Ni filter (21 μ thick) and pulse-height analyzer.

b. Photographic Patterns. In Figure 2 are shown the SAXS patterns for the SI-L specimens taken with X-ray beams parallel (a) and perpendicular (b) to the film sur-

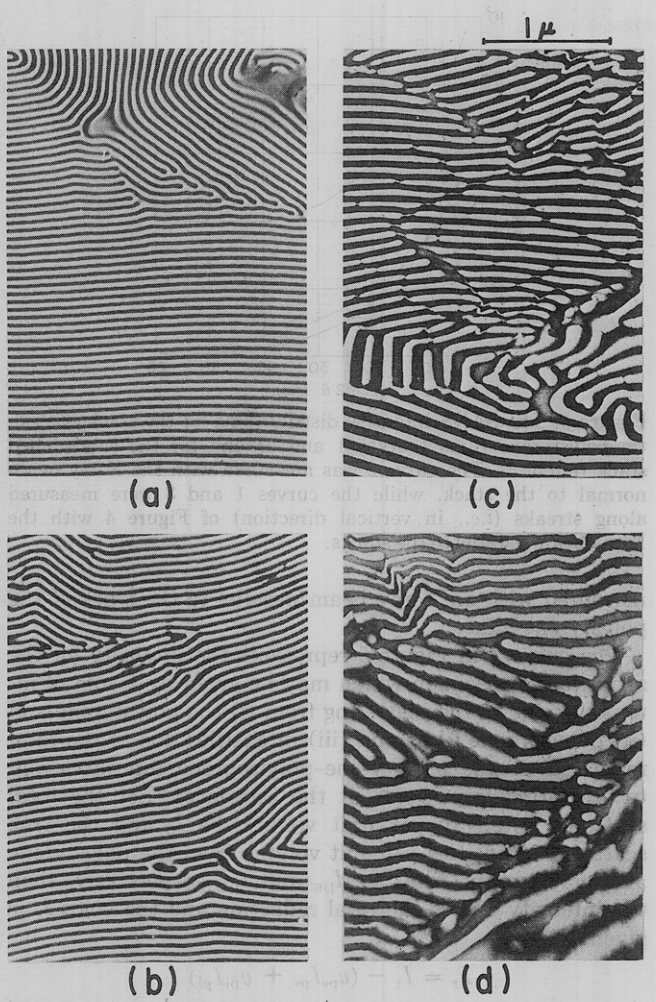

Figure 1. Electron micrographs of ultra-thin sections of the SI-L (a and b) and the SI-H (c and d) films cast from 5% toluene solutions and stained by osmium tetroxide: (a,c) *as*-cast films, (b,d) films annealed at 108°.

faces as shown in the figure. The sharp meridional scattering having many scattering maxima along the direction perpendicular to the film surfaces (Figure 2a) and the circular type diffuse scattering (Figure 2b) indicate that the lamellae are highly oriented with their boundaries parallel to the film surfaces but randomly oriented with respect to the direction normal to the film surfaces.

In Figure 3 are shown the SAXS patterns for the SI-H specimens taken in the same way as in Figure 2. The meridional scattering is less sharp than that of the SI-L specimens, indicating that the orientation of the domains is less perfect for the SI-H specimens than for the SI-L specimens, though the domain still tends to orient parallel to the film surfaces. There are no clear scattering maxima observed in the meridonal scattering of the SI-H specimens, indicating that the uniformity of the domain size and the regularity of the mutual arrangement of the domains are less for the SI-H than for the SI-L. The differences of the domain structures between the SI-H and the SI-L as observed by the SAXS patterns are well confirmed by the electron micrographs shown in Figure 1.

c. Effect of Total Reflection. Since the thickness of a film specimen is very thin, the scattering experiments were performed by stacking the film specimens to a suitable thickness. In this case one should note that the total reflection of X-rays may occur at specimen–air interfaces when the X-ray beam is irradiated parallel to the surfaces of the stack. The total reflection may then affect the meridional scattering intensity distributions shown in Figures 2a and 3a, especially, at small scattering angles.

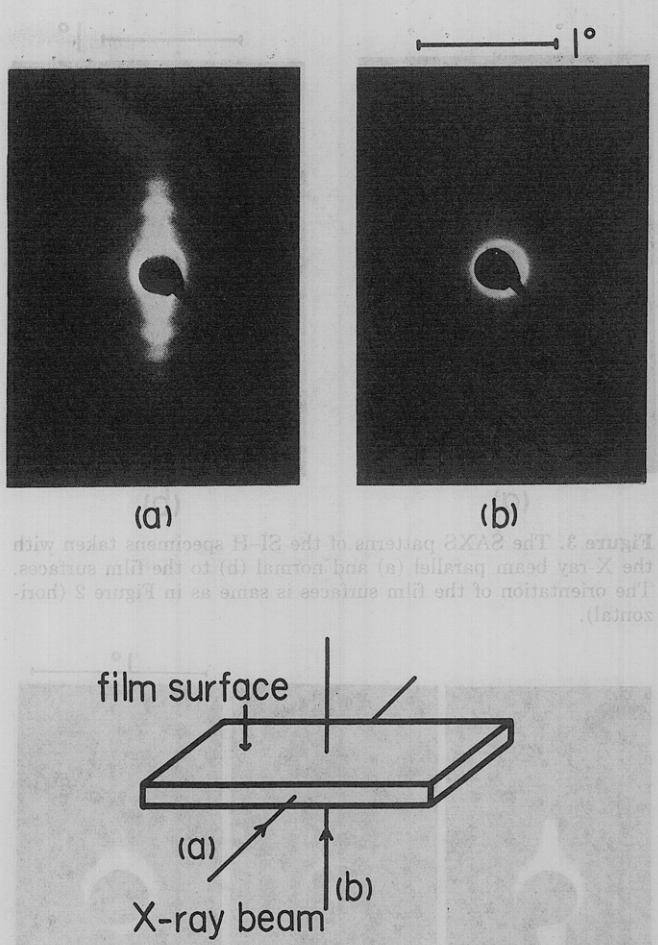

Figure 2. The SAXS patterns of the SI-L specimens taken with the X-ray beam parallel (a) and normal (b) to the film surfaces.

The critical angle of incidence θ_c for the total reflection to occur can be estimated;[11a] for Cu K_α radiation, the values of θ_c for polyisoprene–air and polystyrene–air interfaces are approximately 8.15 and 8.70 min, respectively, assuming that the densities of polyisoprene and polystyrene are 0.925 and 1.052 g per cm^3, respectively. Therefore the effect may be important at 2θ smaller than *ca.* 17 min. If one replaces the air phase with the polyisoprene phase, the value of θ_c for the polystyrene–polyisoprene interfaces is reduced to approximately 1.4 min so that the effect is expected to be very much reduced. It should be noted that the total reflection is, of course, dependent upon smoothness of the surfaces or the interfaces. Therefore the above figures should be regarded as approximate values.

The effect of the total reflection on the SAXS was examined by using thin films of atactic homo-polystyrene. The films were prepared by pressing the melts (*ca.* 100 μ) thick at 190° for 20 min followed by subsequent cooling at a natural rate under a laboratory hot plate, and were checked to be optically isotropic by measuring birefringence.

In Figure 4 are shown the SAXS patterns for a stack of the polystyrene films where patterns a and b were taken with an X-ray beam parallel and perpendicular to the film surfaces, respectively, while pattern c was taken in the same way as pattern a except for a fact that the polystyrene films were now sandwiched with polyisoprene films in order to replace the polystyrene–air interfaces with polystyrene–polyisoprene interfaces.

As seen in the figure, pattern b is a circular-type diffuse

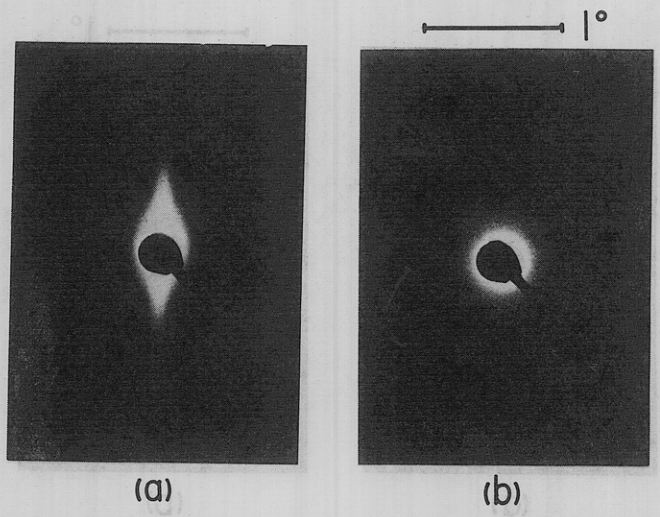

Figure 3. The SAXS patterns of the SI-H specimens taken with the X-ray beam parallel (a) and normal (b) to the film surfaces. The orientation of the film surfaces is same as in Figure 2 (horizontal).

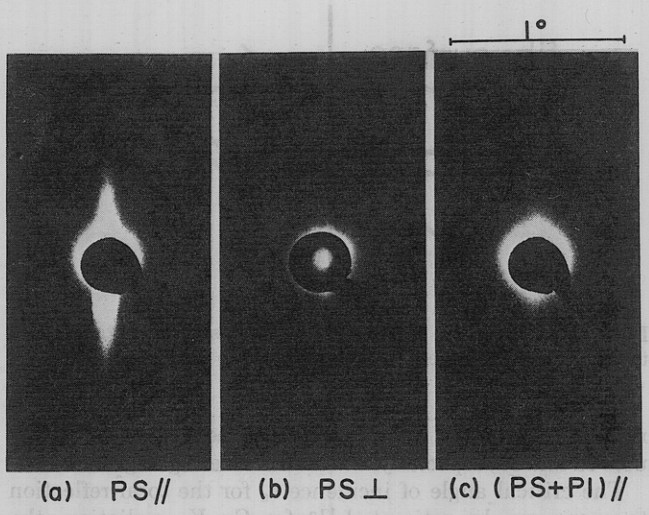

Figure 4. The SAXS pattern of the stack of thin atatctic polystyrene films (a) and that of the sandwiched stack of the polystyrene and polyisoprene films (c). Patterns a and c are taken with the X-ray beam parallel to the stacks whose surfaces are oriented in horizontal, while pattern b is taken with the X-ray beam normal to the film surfaces.

pattern characteristic of systems having isotropic electron density fluctuations. On the other hand, pattern a has strong streaks in a direction perpendicular to the film surfaces. If the polystyrene films are isotropic, patterns a and b should be identical. Therefore the streaks may arise from the total reflection at the polystyrene–air interfaces.[11b] This is confirmed in pattern c, where the total reflection is reduced upon replacing the polystyrene–air interfaces with polystyrene–polyisoprene interfaces, and therefore the streaks are seen to disappear.

The effect of the total reflection on the SAXS may be demonstrated more quantitatively by measuring the intensity distributions by using the counter. This is illustrated in Figure 5 where the curves 1 and 3 correspond to the intensity distributions along the vertical direction of Figures 4a and 4c, respectively, while curve 2 corresponds to that of Figure 4b. The intensity in the ordinate indicates relative intensity per unit volume corrected for air scattering. It is seen, by comparing curves 1 and 2, that the apparent scattered intensity from the polystyrene films (curve 1) almost entirely arises from the total reflection but not from true scattering when the intensity is

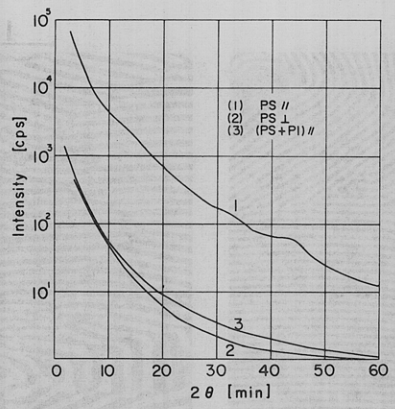

Figure 5. The SAXS intensity distributions for the stack of atactic polystyrene films (curves 1 and 2) and for the sandwiched stack (curve 3). The curve 2 was measured with the X-ray beam normal to the stack, while the curves 1 and 3 were measured along streaks (*i.e.*, in vertical direction) of Figure 4 with the X-ray beam parallel to the stacks.

measured with an X-ray beam parallel to the stack of the polystyrene films.

The curve 3 in Figure 5 represents the intensity for the sandwiched specimen which may be given by a sum of intensities due to the scattering from (i) the polystyrene and (ii) polyisoprene films and (iii) intensities due to the total reflection at the polystyrene–polyisoprene interfaces and to scattering from voids at the interfaces. Let the total scattered intensity per unit volume be I_t and the true scattered intensities per unit volume from the polystyrene and polyisoprene films be I_{ps} and I_{pi}, respectively, then the intensity due to the total reflection and the voids I_r is given by

$$I_r = I_t - (v_{ps}I_{ps} + v_{pi}I_{pi})$$

where v_{ps} and v_{pi} are volume fractions of polystyrene and polyisoprene films in the sandwiched specimens, respectively.

In Figure 6 is shown a result of the evaluated I_r (curve 3), *i.e.*, the remaining contribution of the total reflection and voids to the SAXS for the sandwiched specimens. The curves 1 and 2 represent the I_t and the true scattering from the polystyrene and polyisoprene films, respectively, where values of I_{ps} and I_{pi} were evaluated with X-ray beam normal to the respective films.

As seen in the figure, the effect of the total reflection can be reduced very much by using the sandwiching method down to the level of 300 to 1 counts/sec in a range of 2θ from 5 to 40 min, while for the original stacked specimens it is very large, estimated to be the amount obtained by subtracting the curve 2 from the curve 1 in Figure 5, *i.e.*, 24,000 to 70 counts/sec in the same range of 2θ.[11c] For our purposes, the remaining contribution of the I_r is negligibly small compared with the scattering power of the block copolymers, so that upon sandwiching the contribution of the total reflection can be eliminated practically.

d. The SAXS Intensity Distributions for the *as*-Cast Specimens. In Figure 7 are shown the SAXS intensity distributions along the meridional direction, *i.e.*, a direction normal to the film surfaces (Figure 2) for the SI-L specimens. The solid and broken lines are those uncorrected and corrected for the total reflection, respectively. The uncorrected curve was obtained with the stack of thin copolymer films, while the corrected one was obtained with the stack sandwiched between the polyisoprene films. The total scattered intensity (I_t) of the sandwiched specimens was corrected to obtain the true scattering intensity per unit volume (I_b) of the block copolymer films

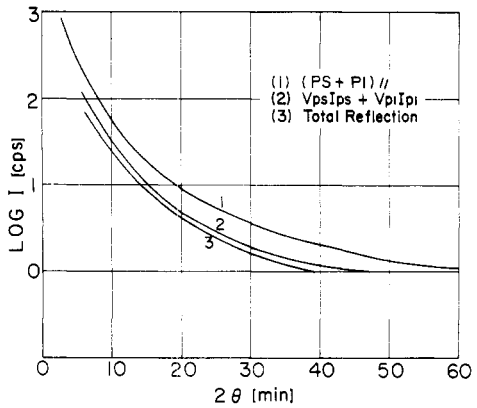

Figure 6. The contribution of the total reflection plus microvoid in the sandwiched specimens.

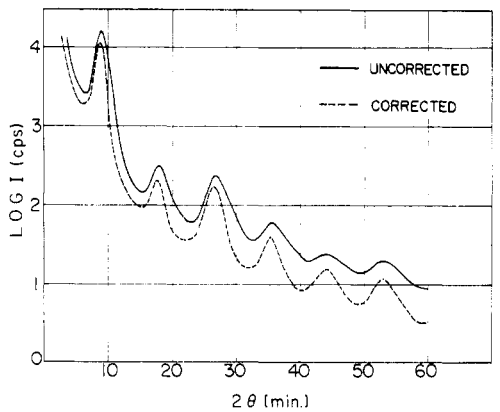

Figure 7. The uncorrected and corrected meridional scattering curves of the SI-L specimens for the total reflection.

by using following relationship

$$I_b = (I_t - v_{pi}I_{pi} - I_r)/v_b$$

where v_b is the volume fraction of the copolymer films in the sandwich.

By comparing curve 3 of Figure 6 and the corrected curve of Figure 7 it is indicated that the value of I_r for the sandwiched specimens is negligibly small compared with the value of I_b for the block copolymer. Therefore the true intensity I_b is given with a good accuracy by $I_b = (I_t - v_{pi}I_{pi})/v_b$. The difference of the intensities between the solid and broken curves arises from the total reflection involved in the stack which is not sandwiched between the polyisoprene films. Surfaces of the copolymer films are much more rough than those of the homopolystyrene films, so that the total reflection power of the copolymer films is expected to be less than the homo-polystyrene films as seen by comparing Figures 5 and 7.

The meridional scattering is accompanied by, at least, seven scattering maxima, each peak of which is related to the first- and higher order diffractions of periodic electron density fluctuations (Figure 7). The single identity period of the density fluctuation is evaluated to be 590 Å by using Bragg's equation, the value of which is in excellent agreement with the average repeat distance, *i.e.*, sum of the thicknesses of a pair of polyisoprene and polystyrene lamellae, as observed from the electron micrographs (580 Å). In contrast to the meridional scattering, the intensity observed with X-ray beam normal to the film surfaces is very weak and continuously decreases with increasing scattering angles as shown in Figure 8. The scattering is independent of the azimuthal angle as expected from Figure 2b.

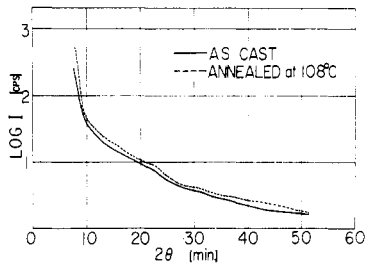

Figure 8. The SAXS intensity distributions for the *as*-cast and annealed SI-L specimens measured with the X-ray beam normal to the film specimens.

The above observations for the SI-L specimens indicate that (i) the domain structure is quite regular so as to exhibit at least seven scattering maxima, and that (ii) the lamellar domains are highly oriented with their boundaries between polystyrene and polyisoprene phase parallel to the film surfaces. It is also indicated by comparing Figures 7 and 8 with Figure 3 (the SAXS patterns for the SI-H specimens) that the domain structure and the macroscopic orientation of the domains become less regular and less perfect with increasing molecular weight.

The effect of molecular weight on the regularity of the domain structure and on the perfection of the domain orientation may be interpreted to arise primarily from an effect of molecular weight on viscosity of the copolymer solutions. The size and mutual distances of the domains formed at the critical micelle concentration must shrink during the solvent evaporation process. The process involves diffusion of the molecules so that the molecules tend to be accomodated in a new equilibrium state. The diffusion of the molecules very much depends upon the viscosity of the copolymer solutions which, in turn, depends upon molecular weight of the copolymer. It is conceivable that the structural regularity observed in the solid films depends upon the extent to which the molecular motion can occur within a given time during the solvent evaporation process.

e. Effect of Annealing. In Figure 9a is shown the effect of annealing on the meridional SAXS intensity distributions for the SI-L specimens. The curves are those corrected for the air scattering and for the total reflection. By comparing the broken curve of Figure 7 with the curves of Figure 9a, it is indicated that annealing at temperatures below T_g of the polystyrene block hardly affect the SAXS intensity distributions. The identity period remains almost constant (590 Å) but the relative peak heights change a little upon annealing at 80°. The change will be shown to arise from the change of volume fraction of the A and B lamellae in next section.

The annealing at temperatures above T_g (*e.g.*, at 108 and 126°) remarkably affect the SAXS curves in terms of both the identity period and the scattering intensity profile; the identity period increases to 660 Å, the relative peak heights and thus volume fractions of A and B lamellae change, and the number of peaks observed (at least 8) increases upon annealing at temperatures above T_g. It should be noted that the intensity of the SAXS measured with X-ray beam normal to the film surfaces does not appreciably change upon annealing at temperatures below and above the T_g as shown in Figure 8, while that of the meridional SAXS appreciably decreases upon annealing at temperatures above T_g.

The decrease of the scattering power can be intepreted as resulting from a decrease of magnitude of electron density fluctuations. This occurs because the thickness of each lamellar increases roughly by the same amount as will be

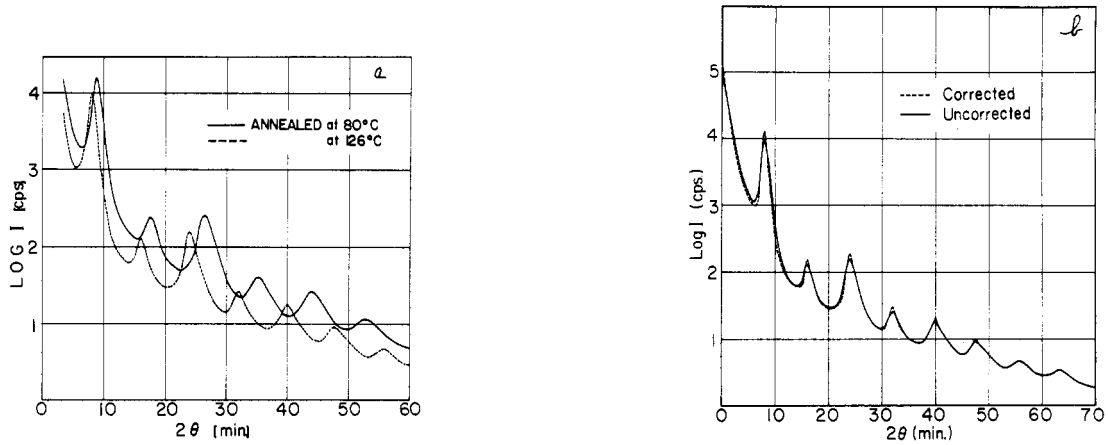

Figure 9. (a) The corrected meridional SAXS intensity distributions for the SI-L specimens annealed at 80 and 126°. (b) The effect of the collimation error due to the slit breadth on the meridional scattering intensity distribution for the SI-L specimens annealed at 126°. The solid and broken curves are those uncorrected and corrected for the slit smearing effect, respectively. Both curves are corrected for the total reflection and air scattering.

shown in the next section. This is also confirmed by close observations of the electron micrographs (Figure 1).

The general tendency of the effect of annealing indicates that (i) annealing at temperatures below T_g of the polystyrene blocks hardly affects the domain structure and that (ii) annealing at temperatures above the T_g increases the regularity of the domain and affects the intensity distributions in terms of positions (Bragg angles), heights, breadths, and number of peaks. It should be pointed out that the intensity distributions are almost identical with that obtained upon annealing at 126° irrespective of the temperatures of annealing if the annealing temperatures are above the T_g of the polystyrene block. This indicates that the change of the domain structure in a temperature range covered in this work (*i.e.*, from *ca.* 25 to *ca.* 180° occurs as a result of the onset of microbrownian motion of the plastic component of the block copolymers.

The domain structure observed in the solid films is not necessarily formed through a thermodynamic equilibrium process, since aspects of the domain structure may be fixed when the solvent levels falls to such a value that the polystyrene glass transition temperature is 30° (the evaporation temperature). Subsequently further solvent is removed, but the system cannot reach equilibrium. On the other hand, after heating above the T_g of polystyrene, the extra strain in the *as*-cast films may be relaxed, and the system is transformed into a thermodynamically more stable state. The shrinking of the sizes and mutual distances of the domains during the solvent evaporation process may be regarded as the most probable process leading to the nonequilibrium states.

Theoretical Analyses

As discussed on the experimental results, the polystyrene-polyisoprene A-B-type block copolymer films cast from toluene solution have the domain structure composed of alternating lamellae of A and B blocks whose domain boundaries are oriented almost perfectly parallel, especially for the SI-L specimens, to the film surfaces. The thicknesses of A and B lamellae which are shown to be around a few hundred ångstroms are quite small compared with the lateral sizes of the lamellae, *i.e.*, the sizes of the lamellae parallel to the boundaries which are seen to be about several thousand ångstroms. Therefore the meridional scattering intensity distributions shown in Figures 7 and 9 can be analyzed quantitatively on the basis

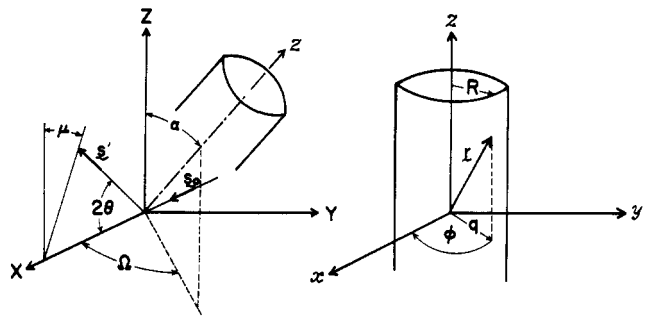

Figure 10. The model used for the theoretical analyses of the experimental scattering intensity distributions.

of models currently proposed for crystalline polymers having one-dimensional electron density variations.[12-16]

Model. In Figure 10 is shown the model considered in this study. The shape of the grain is assumed to be cylindrical having radius R and length NX, where X is the average repeat distance of a pair of A and B lamellae, and N is the number of the repeat unit in the grain. The grain is oriented with respect to the Z axis with orientation distribution function $W(\alpha,\Omega)$. The axes X and Z are taken in the direction parallel to the propagation direction of the incident X-ray beam whose unit vector is defined as $\mathbf{s}_0$, and in the direction normal to the film surfaces, respectively. The SAXS is observed as a function of Bragg angle 2θ and azimuthal angle μ, where $\mathbf{s}'$ is a unit vector along scattered X-ray beam.

The coordinate xyz is the one fixed to the grain in which the domain boundaries of A and B lamellae are oriented perpendicular to the z axis. It is assumed that the electron density variation along the z axis is independent of that along the direction perpendicular to the z axis. Therefore the electron density $\rho(\mathbf{r})$ within the grain is given in a form of

$$\rho(\mathbf{r}) = \rho_1(z)\rho_2(q\cos\phi, q\sin\phi) \quad (1)$$

The variation of electron density along the z axis ($\rho_1(z)$) is approximately given by a trapezium density profile as shown in Figure 11, where the abscissa is coincident with the z axis, and the ordinate shows the excess electron density $\rho_0 = \rho_{st} - \rho_{ip}$ (ρ_{st} and ρ_{ip} being the electron densities of the polystyrene and polyisoprene lamellae, respectively). In our case the phase having higher and lower electron densities are associated with polystyrene and polyisoprene

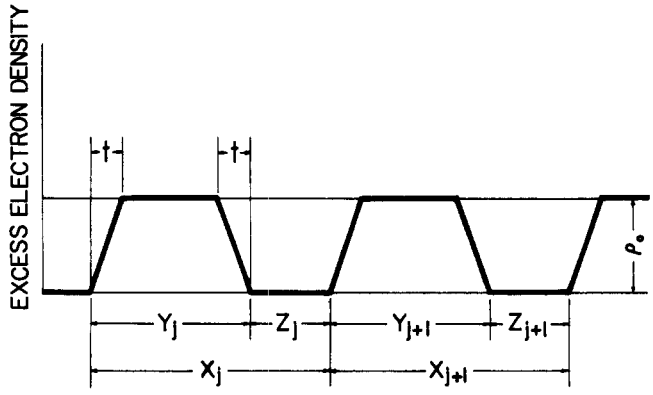

Figure 11. The model of trapezoidal electron density variation for the domain structure.

lamellae, respectively. The lengths Y_j and Z_j are those of the respective phase, and X_j is total length (the repeat distance) of the j-th pair. The length t of the transition region is assumed to be constant, while the length Y_j and Z_j and therefore X_j are assumed to fluctuate independently from the average values, $\bar{Y}$, $\bar{Z}$, and $\bar{X}$.

The length t should depend upon a degree of partial mixing of incompatible A and B block chains at the boundaries and/or upon density distributions of the A and B blocks around their chemical junction points.[5-7,10] The transition region must be energetically less stable than the regions assumed to have constant densities in Figure 11, the contribution of which is proposed to involve the "grain boundary" relaxation mechanism to mechanical relaxation properties of the block and graft copolymers by Soen and Kawai *et al.*[17,18] The "grain boundary" relaxation is believed to be the one associated with cooperative motion of block segments and of backbone and grafted segments in the transition region. Since the term "grain" is used to designate the region in which the orientation of the domains is coherent by Price and Lewis[19,20] and by the present authors in this paper, it seems better to use the term "domain boundary" instead of the "grain boundary" in order to describe phenomena related to molecular motion in the transition region.

Calculations. Let the unit vectors along X, Y, Z, x, y, and z be **i**, **j**, **k**, **i**′, **j**′, and **k**′. The relationship between the (**i**, **j**, **k**) and (**i**′, **j**′, **k**′) coordinates is given by

$$\begin{pmatrix} \mathbf{i} \\ \mathbf{j} \\ \mathbf{k} \end{pmatrix} = \begin{pmatrix} \sin\Omega & \cos\alpha\cos\Omega & \sin\alpha\cos\Omega \\ -\cos\Omega & \cos\alpha\sin\Omega & \sin\alpha\sin\Omega \\ 0 & -\sin\alpha & \cos\alpha \end{pmatrix} \begin{pmatrix} \mathbf{i}' \\ \mathbf{j}' \\ \mathbf{k}' \end{pmatrix} \quad (2)$$

Amplitude of scattering $a(\mathbf{s})$ from a given grain oriented at α and Ω with respect to the XYZ coordinate is given by

$$a(\mathbf{s}) = \int_V \rho(\mathbf{r}) \exp[-2\pi i \mathbf{r}\cdot\mathbf{s}]dV \quad (3)$$

where $\rho(\mathbf{r})$ is given by eq 1. The electron density variation ρ_2 should be very small compared with that ρ_1, so that ρ_2 may be assumed to be constant, *i.e.*, $\rho_2 = \rho_0'$. Therefore eq 1 is rewritten as

$$\rho(\mathbf{r}) = \rho_0'\rho_1(\mathbf{z}) \quad (4)$$

The vector **s** is the scattering vector defined by

$$\mathbf{s} = (\mathbf{s}' - \mathbf{s}_0)/\lambda$$
$$= (1/\lambda)[(1 - \cos 2\theta)\mathbf{i} + (\sin 2\theta \sin\mu)\mathbf{j} + (\sin 2\theta \cos\mu)\mathbf{k}] \quad (5)$$

and the vector **r** is given by

$$\mathbf{r} = (q\cos\phi)\mathbf{i}' + (q\sin\phi)\mathbf{j}' + z\mathbf{k}' \quad (6)$$

Now from eq 2 to 6, it follows that

$$a(\mathbf{s}) = a_l(\mathbf{s})a_b(\mathbf{s}) \quad (7)$$

where

$$a_l(\mathbf{s}) = \int_0^R \int_0^{2\pi} \rho_0' \exp[-2\pi i q(s_1\cos\phi + s_2\sin\phi)]q\,dq\,d\phi \quad (8)$$

$$a_b(\mathbf{s}) = \int \rho_1(z) \exp[-2\pi i s_3 z]dz \quad (9)$$

$$s_1 = (1/\lambda)[(1 - \cos 2\theta)\sin\Omega - \sin 2\theta \sin\mu\cos\Omega]$$
$$s_2 = (1/\lambda)[(1 - \cos 2\theta)\cos\alpha\cos\Omega + \sin 2\theta \sin\mu\cos\alpha\sin\Omega - \sin 2\theta\cos\mu\sin\alpha]$$
$$s_3 = (1/\lambda)[(1 - \cos 2\theta)\sin\alpha\cos\Omega + \sin 2\theta \sin\mu\sin\alpha\sin\Omega + \sin 2\theta\cos\mu\cos\alpha] \quad (10)$$

and λ is the wavelength of X-ray beam.

In eq 7, the term $a_l(\mathbf{s})$ is associated with the lateral size of the grain, while the term $a_b(\mathbf{s})$ is associated with domain structure within the grain; ρ_0, t, the distribution of the lengths Y_j and Z_j, and N. Equation 8 can be easily integrated to give

$$a_l(\mathbf{s}) = 2(\pi R^2)J_1(W)/W \quad (11)$$

where $W = 2\pi RA/\lambda$, and $A = [s_1^2 + s_2^2]^{1/2}$. $J_1(W)$ is the Bessel function of the first kind of order one. The average scattered intensity per unit volume is then given by

$$I(2\theta,\mu) = K\left(\frac{\pi R^2}{NX}\right)\int_0^{\pi}\int_0^{2\pi}\left[\frac{J_1(W)}{W}\right]^2 |a_b(\mathbf{s})|^2 \times W(\alpha,\Omega)\sin\alpha\,d\alpha\,d\Omega \quad (12)$$

where K is a constant related to the absolute intensity. As discussed earlier, we may assume as a first approximation that the grain is perfectly oriented parallel to Z axis. In this case the meridional scattering intensity (*i.e.*, intensity at $\mu = 0°$) is simply given by

$$I(2\theta) = K\left(\frac{\pi R^2}{NX}\right)\left[\frac{J_1(W)}{W}\right]^2 |a_b(\mathbf{s})|^2 \quad (13)$$

where $W = \pi R(2\sin\theta)^2/\lambda^2$, $s = (\sin 2\theta)/\lambda$.

The term $a_b(s)$ in eq 13 has been currently calculated by Blundell,[12,13] and Tsvankin *et al.*[14-16] for the system having one-dimensional electron density variation as in Figure 11. In this paper we shall analyze the experimental intensity distributions based upon eq 13 and by using Blundell's model for the term $|a_b(s)|^2$.

Blundell's Model for $|a_b(s)|^2$. Blundell[13] assumed that the variation of the lengths Y_j and Z_j are independent and are given by symmetric Gaussian functions with the respective mean lengths of $\bar{Y}$ and $\bar{Z}$, and the standard deviations σ_y and σ_z;

$$H(Y_j) = (2\pi)^{-1/2}\sigma_y^{-1}\exp[-(Y_j - \bar{Y})^2/2\sigma_y^2] \quad (14a)$$

$$h(Z_j) = (2\pi)^{-1/2}\sigma_z^{-1}\exp[-(Z_j - \bar{Z})^2/2\sigma_z^2] \quad (14b)$$

The mean periodic distance $\bar{X}$ and the standard deviation σ_x for the variation of X_j are given by $\bar{X} = \bar{Y} + \bar{Z}$, and $\sigma_x^2 = \sigma_y^2 + \sigma_z^2$. The volume fraction of polystyrene phase (χ) is given by $\chi = (\bar{Y} - t)/\bar{X}$.

According to the model, the term $|a_b(s)|^2/NX$ is shown to be given by[12]

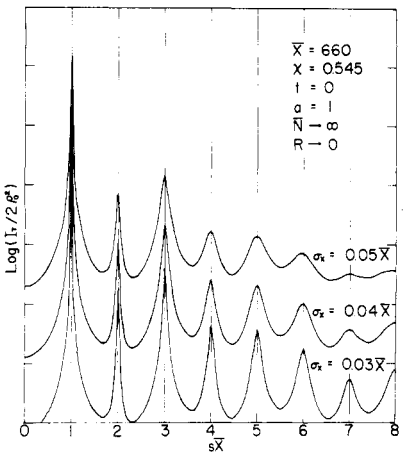

Figure 12. The effect of σ_x on the calculated meridional scattering curves.

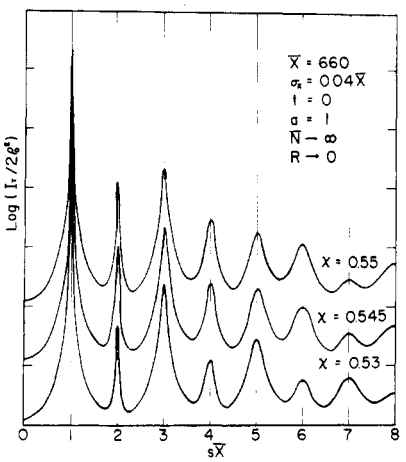

Figure 13. The effect of χ on the calculated meridional scattering curves.

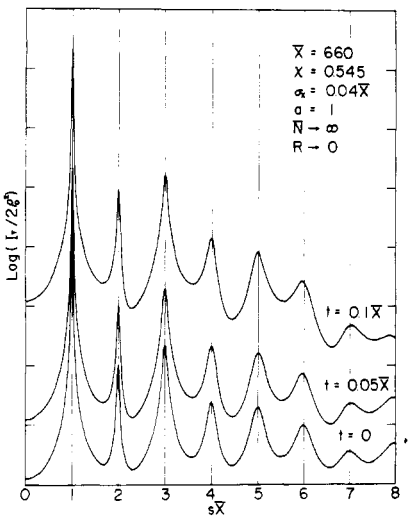

Figure 14. The effect of t on the calculated meridional scattering curves.

$$|a_h(s)|^2/(N\bar{X}) = I_B(s) - I_C(s) \tag{15}$$

where the term $I_B(s)$ is associated with the first- and higher order scattering maxima, while the term $I_C(s)$ is associated with the zero-order scattering. The term I_B was calculated for the trapezoidal model by Blundell, the result of which is shown in eq 2 of his paper.[13] Since Blundell did not calculate the term I_C for the model, we calculated the term in order to estimate roughly the length of the grain $N\bar{X}$, the result of which is given by

$$I_C(s) = \frac{2}{N\bar{X}}\left(\frac{\rho_0}{2\pi s}\right)^2\left[\frac{\sin(\pi st)}{\pi st}\right]^2 \times \frac{I_{C1}}{[1 - 2|F_x|\cos(2\pi s\bar{X}) + |F_x|^2]^2} \tag{16}$$

$$I_{C1} = \mathrm{Re}(A) - |F_x|^N\{\mathrm{Re}(A)\cos(2\pi sN\bar{X}) + \mathrm{Im}(A)\sin(2\pi sN\bar{X})\} \tag{17}$$

$$\begin{aligned}\mathrm{Re}(A) = &-|F_x|(|F_y| + |F_x||F_z|)\cos[2\pi s(1+\chi)\bar{X}] + \\ &2|F_x|(1 + |F_x|^2)\cos(2\pi s\bar{X}) - \\ &(|F_z| + |F_x|^3|F_y|)\cos[2\pi s(1-\chi)\bar{X}] + \\ &2|F_x|(|F_x||F_y| + |F_z|)\cos(2\pi s\chi\bar{X}) - 4|F_x|^2\end{aligned} \tag{18}$$

$$\begin{aligned}\mathrm{Im}(A) = &|F_x|(|F_y| - |F_x||F_z|)\sin[2\pi s(1-\chi)\bar{X}] - \\ &2|F_x|(1 - |F_x|^2)\sin(2\pi s\bar{X}) + \\ &(|F_z| - |F_x|^3|F_y|)\sin[2\pi s(1-\chi)\bar{X}] - \\ &2|F_x|(|F_x||F_y| - |F_z|)\sin(2\pi s\chi\bar{X})\end{aligned} \tag{19}$$

and the terms $|F_x|$, $|F_y|$, and $|F_z|$ are defined by

$$|F_y| = \exp(-2\pi^2 s^2\sigma_y^2)$$
$$|F_z| = \exp(-2\pi^2 s^2\sigma_z^2)$$
$$|F_x| = |F_y||F_z|$$

The quantity s is defined by $s = (\sin 2\theta)/\lambda$.

From eq 13, 15, and 16 the meridional scattering is seen to depend upon the structure parameters, $\bar{X}$, χ, σ_y, σ_z, t, and N, as well as the lateral dimension (radius R) of the grain. The parameters R and N are apparently associated with size of the grain, while the other parameters are associated with the internal domain structure.

In order to evaluate quantitatively these parameters, one should take into account the orientation distribution ($W(\alpha,\Omega)$) of the grain and the collimation errors due to slit height and slit breadth on the meridional scattering intensity distribution. We shall, however, restrict our treatment to the system where the grain is perfectly oriented for a qualitative evaluation of the structure parameters. For the perfectly oriented system, the collimation error due to the slit height would not affect the intensity distribution since the surfaces of the film specimens were set parallel to the long direction of the slit. Based upon the assumption, we neglected the correction for the error due to the slit height, but corrected for the error due to the finite breadth of the slit after the method given by Kratky, Porod, and Skala.[21] In Figure 9b is shown the effect of the correction for the collimation error due to the slit breadth on the meridional scattering intensity. The error is seen to affect only a little the intensity distribution as discussed by Kratky, Porod, and Skala.

Calculated Results and Comparison with the Experimental Results

The calculated results are shown in Figures 12–18 where logarithm of relative scattered intensity was plotted as a function of the reduced scattering angle $s\bar{X} = 2(\bar{X}/\lambda)\sin\theta$. At first we shall consider only the term $I_B(s)$ associated with the first- and higher order scattering maxima, and then the terms $I_C(s)$ and $[J_1(W)/W]^2$ associated with zero-order scattering. The calculated results will be compared with the SI-L specimens only, since the SI-H specimens exhibit no clear scattering maxima.

The structural parameters χ, $\bar{X}$, t, σ_x, a, R, and N were

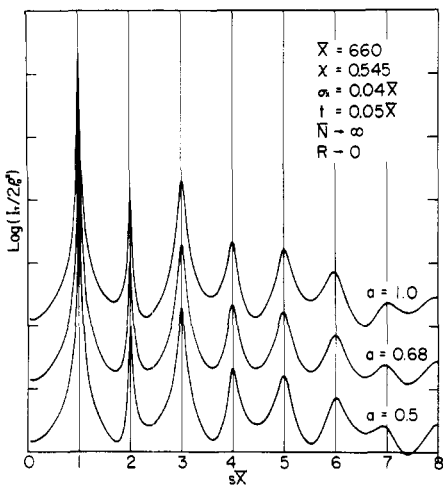

Figure 15. The effect of $a(=(\sigma_y/\sigma_z)(\bar{Z}/\bar{Y}))$ on the calculated meridional scattering curves.

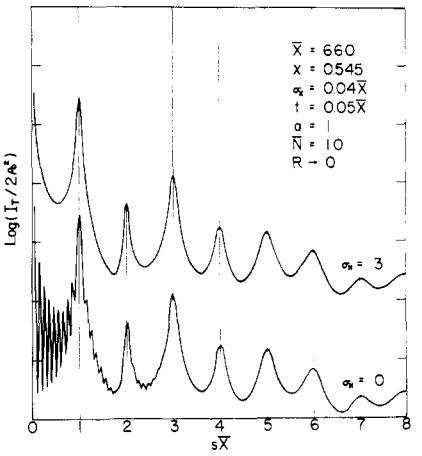

Figure 16. The effect of the grain length N on the calculated meridional scattering curves.

estimated by a trial and error method. However estimation of these parameters was fairly simple and accurate, since the parameters affect the SAXS intensity distribution sensitively in different ways as will be seen below. It should be pointed out that the estimation of t itself may be performed more accurately with the method proposed by Ruland[22] and Vonk[23] based upon analyses of systematic deviation of the SAXS intensity distribution from the Porod's law[28] than with the method employed in this report. This work is now being carried out in our laboratory.

In Figure 12 is shown the effect of σ_x, fluctuation in the identity period, under a given set of parameters $\bar{X}$ = 660 Å, χ = 0.545, t = 0, and a = 1. The shape of grain is given by $\bar{N} = \infty$, and R = 0, so that only the I_B term is nonzero. The quantity a is a parameter characterizing the relative magnitude of fluctuations in terms of thicknesses of polystyrene (σ_y) and polyisoprene (σ_z) lamellae; $(\sigma_y/\bar{Y}) = a(\sigma_z/\bar{Z})$. Therefore, σ_y becomes a little greater than σ_z in case of a = 1 for the SI-L specimens, since $\bar{Y}$ is expected to be a little greater than $\bar{Z}$ as expected from the chemical composition. The value of $\bar{X}$ is predetermined from positions of scattering maxima; $\bar{X}$ = 660 and 590 Å with an error of less than 1% for the copolymer films annealed above and below T_g of polystyrene block, respectively. It is seen that the value of σ_x sensitively affects the number of scattering maxima and half-breadth of the peak. By comparing with the experimental scattering intensity, the values of σ_x are seen to be about 0.04 $\bar{X}$ and 0.05 $\bar{X}$ with an error of less than 10% for the copolymers annealed above and below the T_g, respectively, indicating that the annealing above the T_g improves structure regularity.

In Figure 13 is shown the effect of parameter χ (the volume fraction of polystyrene phase) on the scattering curve for a given set of parameters; $\bar{X}$ = 660 Å, $\sigma_x = 0.04\bar{X}$, t = 0, a = 1, $\bar{N} = \infty$, and R = 0. The values of χ are seen to affect sensitively the relative peak heights. As the value of χ approaches to ½, the second and the fourth peak heights become small compared with the third and the fifth peak heights, respectively. By comparing with the experimental curves, the values of χ are about 0.56 and 0.54 with an error of less than *ca.* 1% for the *as*-cast and annealed films above the T_g, respectively. Therefore the annealing increases thicknesses of both polystyrene and polyisoprene lamellae, but polyisoprene lamellae tend to expand more than the polystyrene ones, the tendency of which is seen by close observations of the micrograph (Figure 1). The tendency is more clearly seen for the SI-H specimens, the copolymers having higher molecular weight. Although there is a little change in the value of χ upon annealing at 80°, the appreciable change does not occur unless the annealing temperature is higher than the T_g. It is not well understood at present why the lamellar thickening occurs and why the volume fraction χ changes upon annealing above the T_g of polystyrene.

In Figure 14 is shown the effect of thickness of the domain boundary region t on the scattering curves. The quantity t affects the scattering curve through the factor $\sin^2(\pi st)/(\pi st)^2$, so that the effect becomes increasingly important at higher scattering angles. The factor sensitively decreases the heights of higher order diffraction peaks, especially peaks of order greater than the third as seen in the figure. Therefore upon increasing the value of t, a profile of the intensity distribution becomes the one which decreases more rapidly with increasing scattering angle.

The profiles of the intensity distributions remain almost the same before and after annealing of the SI-L specimens (see Figures 7 and 9a), indicating that the values of $t/\bar{X}$ are hardly affected by the annealing. By comparing the calculated results with the experimental results, the value of $t/\bar{X}$ is roughly estimated to be 0.05 with an error of less than 40%. This indicates that the absolute value of t itself tends to increase upon annealing above the T_g, since the value of $\bar{X}$ increases upon annealing. The increase of the absolute value of t is, however, negligibly small compared with error involved in evaluating $t/\bar{X}$. Thus the values of $t/\bar{Y}$ and $2t/(\bar{Y} - 2t)$ are estimated to be *ca.* 0.08–0.09 and *ca.* 0.2, respectively, for the SI-L specimens both before and after annealing. The absolute value of t is about 30 Å, indicating that there are roughly six monomeric units each in the boundary, since the polyisoprene block has been shown to be in a form of mostly 1,2 or 3,4 addition.[3] The estimated value of $2t/(\bar{Y} - 2t)$ is in fairly good agreement with the value of $(\Delta R/R)$ = 0.18 estimated for styrene–isoprene–styrene triblock copolymer having a spherical domain of radius R and thickness of the transition region ΔR.[18]

The estimated value of boundary thickness t of *ca.* 30 Å is also in rough accord with the prediction of Helfand and Tagami,[24] and Helfand.[25] It should be also pointed out that there are papers[26,27] that attempt to measure the interfaces of the domain structure of the block copolymer by using the SAXS intensity distribution at large angles where the Porod's law[28] is applicable. The authors believe the value of t and thus the effects of annealing and molecular weight of the block copolymer on t are estimated

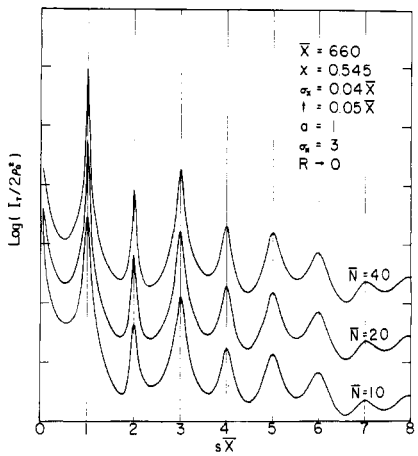

Figure 17. The effect of the grain length N on the calculated meridional scattering curves for a given value of $\sigma_N = 3$.

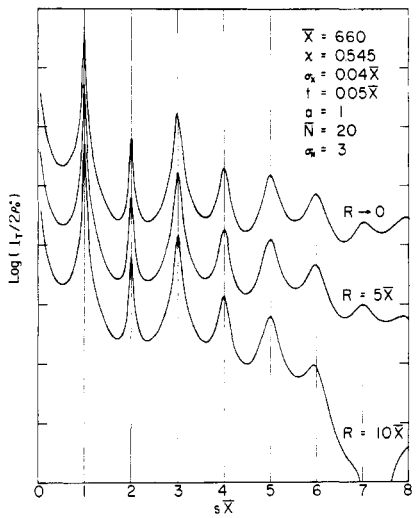

Figure 18. The effect of the lateral size of the grain R on the calculated meridional scattering curves.

more quantitatively by analyzing the systematic deviation from the Porod's law at large scattering angles based upon the theories developed by Ruland[22] and Vonk[23] *et al.* This sort of work is now being carried out.

In Figure 15 is shown the effect of parameter a on the scattering curve where a was defined by $(\sigma_y/\sigma_z) = a(\bar{Y}/Z)$. For the SI-L specimen, the value of $\bar{Y}$ which is given by $\bar{Y} = \chi\bar{X} + t$ is *ca.* $0.6\bar{X}$, so that the case where $a = 1$ corresponds to the case where σ_y is greater than σ_z, while the case where $a \simeq 0.67$ corresponds to the case of $\sigma_y \simeq \sigma_z$. The value of a is shown to affect the shape of the curve around the scattering minima. By comparing with the experimental curves, a reasonable value of a may be found in between the two extremes, suggesting that the fluctuation in the lamellar thickness of polystyrene is greater than that of polyisoprene.

In the calculations made so far, we neglected the zero order scattering, *i.e.*, the terms I_C and $[J_1(W)/W]^2$, so that the intensity approaches zero for $s\bar{X} < 1$. In figures 16–18 are shown the effects of N and R on the scattering curves.

In Figure 16 is shown the effect of N, the length of the grain, on the scattering curve where the value of R is still zero. The lower curve is obtained by setting $N = 10$ exactly ($\sigma_N = 0$), while the upper one is obtained by setting average value of N ($\bar{N}$) as 10 and by giving a discrete symmetrical distribution of $N(P(N))$ with the standard deviation $\sigma_N = 3$

Table I
Some Structure Parameters of the Domain Structure of SI-L Specimens

Structure Parameters	Source of Measurements: Chemical Composition[a]	Electron Microscope	SAXS
a. Specimens Annealed at Temperatures above T_g of Polystyrene Block			
χ (%)	55.5	55.2	54.5
$\bar{x}$ (Å)		666	660
$t/(\bar{y} - 2t)$			0.1
t (Å)			33
$\sigma_x/\bar{X}$			0.04
b. *as*-Cast Specimens			
χ (%)	55.5	56	56
$\bar{x}$ (Å)		580	590
$t/(\bar{y} - 2t)$			0.1
t (Å)			30
$\sigma_x/\bar{X}$			0.05

[a] Calculated by assuming densities of polystyrene and polyisoprene being 1.052 and 0.925 g per cm³, respectively.

$$P(N) = \exp\left\{-\frac{(N-\bar{N})^2}{2\sigma_N^2}\right\} \Big/ \sum_{N=1}^{2\bar{N}-1} \exp\left\{-\frac{(N-\bar{N})^2}{2\sigma_N^2}\right\} \quad (20)$$

Many scattering maxima in the lower curve at scattering angles specified by $s\bar{X} < 3$ are due to the higher order scattering maxima from isolated rodlike grains. The zero-order scattering is indicated to affect the scattering curve only at small angles $s\bar{X} < 3$. The size distribution of the grain smears out the higher order scattering maxima to give smooth distribution of the zero-order scattering. The average value of the term I_C is given by

$$\langle I_C \rangle_{av} = \sum_{N=1}^{2\bar{N}-1} I_C(N)P(N) \quad (21)$$

In Figure 17 is shown the effect of average number $\bar{N}$ on the scattering curve. Comparison with the experimental results gives a qualitative estimation of $\bar{N}$ being of the order of 10, suggesting that the length of the grain is of the order of several thousand ångstroms.

In Figure 18 is shown the effect of the lateral size of the grain R which affects the scattering curves as a multiplied factor on the term $|a_b(s)|^2$ as shown in eq 13. As expected from the equation when R approaches zero, the term $[J_1 \cdot (W)/W]$ approaches unity so that the lateral size does not affect the intensity distribution. For a finite value of R, the term $[J_1(W)/W]$ is unity at $2\theta = 0$, and asymptotically decreases with increasing 2θ, the rate of which depends upon the value of R, greater for greater value of R. Therefore, the effect of R is expected to be increasingly sensitive with increasing 2θ in a manner somewhat similar to the effect of t. This involves a difficulty for quantitative evaluations of the value of t which is of most interest to us. By comparing with the experimental curves, the value of R is seen to be of the order of a thousand ångstroms.

It is roughly estimated by comparing the experimental curves with calculated curves shown in Figures 16–18 that the grain size is of the order of several thousand ångstroms. More accurate evaluation requires, of course, the correction for the collimation error due to slit height, which is now being attempted. Since the size of the grain is fairly large, light-scattering method should be more powerful in estimating the size. This work also is now

being carried out in our laboratory. If the grain size can be accurately estimated by this method, the determination of t can be more accurately performed.

Conclusion

Domain structures of alternating lamellae of styrene and isoprene A–B-type block copolymers were investigated by means of the SAXS and electron microscopic measurements. The results are summarized as follows. (i) The lamellae formed by the microphase separation tend to orient with their boundaries parallel to the bulk film surfaces prepared by solvent casting. (ii) The regularity of the domain structure and perfection of the domain orientation depend upon molecular weight of the copolymers. These are higher for the lower molecular weight copolymers. (iii) Annealing of the *as*-cast specimens at temperatures below T_g of a polystyrene block hardly affects the domain structure, while those at temperatures above the T_g affect the domain structure in terms of the structure requlority (σ_x) and the identity period ($\bar{X}$); the regularity increases and each lamella thickens roughly by the same amount. The change of the domain structure in the temperature range studied is then interpreted to occur as a consequence of the onset of microbrownian motion (at T_g) of the plastic component. (iv) The change of the domain structure upon annealing implies that the domain is not necessarily formed through thermodynamic equilibrium processes. The residual strain in the solid texture may then be relaxed upon annealing, so that a more favorable structure is formed. The change of the domain structure was independent of rate of cooling from the annealed temperature to room temperature. (v) When the SAXS is measured with X-ray beam parallel to surfaces of thin films, one generally has to consider the effect of total reflection at air–film interfaces on the SAXS. This was corrected by adopting a sandwiching method. (vi) The theoretical analyses yielded valuable information on the domain structure of the SI-L specimens. The structure parameters such as χ, $\bar{X}$, t, σ_x, as well as R and N are qualitatively evaluated. These parameters affect the SAXS intensity distributions sensitively in different ways, so that qualitative estimations of them were very fruitful. Some of the results are summarized in Table I. It was also indicated that (a) the fluctuation of the lamellar thickness of polystyrene is greater than that of polyisoprene, and that (b) the size of the grain is about several thousand ångstroms. This fact (a) may be interpreted in terms of easier molecular motion of the isoprene block than that of the styrene block at higher concentrations. The values of χ and $\bar{X}$ measured from different experimental sources agree very well as seen in Table I.

Acknowledgment. The authors acknowledge to Dr. Y. Itoh, Messrs. K. Yoshimura and M. Nishimura, Pioneering Research and Development Laboratories, Toray Industries, Inc., for preparation of the electron micrographs, and to Professor H. Tashiro, Institute for Chemical Research, Kyoto University, for kindly arranging for preliminary measurements of the SAXS. The authors are indebted to Mr. K. Miyoshi, Central Research Laboratories, Mitsubishi Chemical Industries, Inc., for preparing the SI-L block copolymers. We thank Dr. T. Soen, Department of Textile Engineering, Art Industrial and Fiber College of Kyoto, for valuable discussions. This work was supported in part by a grant from the Scientific Research Fund (Kagaku Kenkyu-hi, 743020-1972) of the Ministry of Education, Japan, and by a grant from the Idemitsu Kosan Co., Ltd., Tokyo, Japan, the Mitsui Petrochemical Industries, Ltd., Tokyo, Japan, and the Japan Synthetic Rubber Co., Ltd., Tokyo, Japan.

References and Notes

(1) (a) Published in part in *Rep. Progr. Polym. Phys. Jap.*, 16 (1973); presented partly at the 22nd Symposium on Polymer Chemistry, Japan, Tokyo, Nov 1973. (b) On leave from the Central Research Laboratory, Idemitsu Kosan Co., Ltd., Sodegaura-Cho, Kimitsu-Gun, Chiba-Ken, Japan. (c) On leave from the Research Center, Mitsui Petrochemical Industries, Ltd., Waki-Mura, Kuga-Gun, Yamaguchi-Ken, Japan. (d) Division of Macromolecular Science, Case Western Reserve University, Ohio 44106.
(2) (a) C. Sadron, *Angew Chem.*, **75**, 472 (1963). (b) E. Vanzo, *J. Polym. Sci., Part A-1*, **4**, 1727 (1965).
(3) T. Inoue, T. Soen, T. Hashimoto, and H. Kawai, *J. Polym. Sci., Part A-2*, **17**, 1283 (1969).
(4) T. Uchida, T. Soen, T. Inoue, and H. Kawai, *J. Polym. Sci., Part A-2*, **10**, 101 (1972).
(5) D. J. Meier, *J. Polym. Sci., Part C*, **26**, 81 (1969).
(6) D. J. Meier, *Polym. Prepr., Amer. Chem. Soc., Div. Polym. Chem.*, **11**, 400 (1970).
(7) D. F. Leary and M. C. Williams, *J. Polym. Sci., Part B*, **8**, 335 (1970).
(8) T. Soen, T. Inoue, K. Miyoshi, and H. Kawai, *J. Polym. Sci., Part A-2*, **10**, 1757 (1972).
(9) T. Ono, H. Minamiguchi, T. Soen, and H. Kawai, *Kolloid-Z. Z. Polym.*, **250**, 394 (1972).
(10) D. F. Leary and M. C. Williams, *J. Polym. Sci., Polym. Phys. Ed.*, **11**, 345 (1973).
(11) (a) See, for example, A. Guinier, "X-ray Diffraction in Crystals, and Amorphous Bodies," W. H. Freeman, San Francisco, Calif., 1963. (b) It should be noted that a scattering pattern similar to the pattern a was observed even with a single film specimen and that the scattering appeared as the streaks (the pattern a) were greatly reduced in intensity when the surfaces of the stack was slightly tilted with incident X-ray beam in order to avoid the condition of the total reflection being satisfied. These observations may further confirm that the streak-like scattering of the pattern(a) arises more from the total reflection than from intervening voids between the specimens. (c) The counting rate (counts per second) appearing in this paper corresponds to relative intensities but not to absolute intensities.
(12) D. J. Blundell, *Acta Crystallogr., Ser. A*, **26**, 472 (1970).
(13) D. J. Blundell, *Acta. Crystallogr., Ser. A*, **26**, 476 (1970).
(14) D. Ya. Tsvankin, *Vysokomol. Soedin., Ser. A*, **6**, 2078 (1964).
(15) D. Ya. Tsvankin, *Vysokomol. Soedin., Ser. A*, **11**, 2652 (1969).
(16) V. I. Gerasimov, Ya. V. Genin, A. I. Kitaigorodsky, and D. Ya. Tsvankin, *Kolliod-Z. Z. Polym.*, **250**, 518 (1972).
(17) T. Soen, T. Ono, K. Yamashita, and H. Kawai, *Kolloid-Z. Z. Polym.*, **250**, 459 (1972).
(18) T. Soen, M. Shimomura, T. Uchida, and H. Kawai, submitted to *Kolloid-Z. Z. Polym.*
(19) P. R. Lewis and C. Price, *Polymer*, **12**, 258 (1971).
(20) P. R. Lewis and C. Price, *Macromolecules*, in press.
(21) O. Kratky, G. Porod, and Z. Skala, *Acta Phys. (Budapest)* **13**, 76 (1960).
(22) W. Ruland, *J. Appl. Crystallogr.*, **4**, 70 (1971).
(23) C. G. Vonk, *J. Appl. Crystallogr.*, **6**, 81 (1973).
(24) E. Helfand and Y. Tagami, *J. Polym. Sci., Part B*, **9**, 741 (1971), *J. Chem. Phys.*, **56**, 3592 (1971).
(25) E. Helfand, 166th National Meeting of the American Chemical Society, Chicago, Ill., Sept, *Polym. Prepr.*, **14**, 940 (1973).
(26) D. G. LeGrand, *J. Polym. Sci., Part B*, **8**, 195 (1970).
(27) H. Kim, *Macromolecules*, **5**, 594 (1972).
(28) G. Porod, *Kolloid-Z., Z. Polym.*, **124** (2), 83 (1951); *ibid.*, **125** (1), 51 (1952); *ibid.*, **125** (2), 108 (1952).